Advances in Radiation Oncology (2025) **10**, 101669

advances in radiation oncology

www.advancesradonc.org

Scientific Article

Delta-Radiomics Approach Using Contrast-Enhanced and Noncontrast-Enhanced Computed Tomography Images for Predicting Distant Metastasis in Patients With Borderline Resectable Pancreatic Carcinoma

Takanori Adachi, PhD,[a] Mitsuhiro Nakamura, PhD,[a,b,*] Takahiro Iwai, PhD,[a] Michio Yoshimura, MD, PhD,[a] and Takashi Mizowaki, MD, PhD[a]

[a]*Department of Radiation Oncology and Image-Applied Therapy, Kyoto University, Shogoin, Sakyo-ku, Kyoto, Japan; and* [b]*Department of Advanced Medical Physics, Graduate School of Medicine, Kyoto University, Shogoin, Sakyo-ku, Kyoto, Japan*

Received 24 December 2023; accepted 21 October 2024

Purpose: To predict distant metastasis (DM) in patients with borderline resectable pancreatic carcinoma using delta-radiomics features calculated from contrast-enhanced computed tomography (CECT) and non-CECT images.

Methods and Materials: Among 250 patients who underwent radiation therapy at our institution between February 2013 and December 2021, 67 patients were deemed eligible. A total of 11 clinical features and 3906 radiomics features were incorporated. Radiomics features were extracted from CECT and non-CECT images, and the differences between these features were calculated, resulting in delta-radiomics features. The patients were randomly divided into the training (70%) and test (30%) data sets for model development and validation. Predictive models were developed with clinical features (clinical model), radiomics features (radiomics model), and a combination of the abovementioned features (hybrid model) using Fine-Gray regression (FG) and random survival forest (RSF). Optimal hyperparameters were determined using stratified 5-fold cross-validation. Subsequently, the developed models were applied to the remaining test data sets, and the patients were divided into high- or low-risk groups based on their risk scores. Prognostic power was assessed using the concordance index, with 95% CIs obtained through 2000 bootstrapping iterations. Statistical significance between the above groups was assessed using Gray's test.

Results: At a median follow-up period of 23.8 months, 47 (70.1%) patients developed DM. The concordance indices of the FG-based clinical, radiomics, and hybrid models were 0.548, 0.603, and 0.623, respectively, in the test data set, whereas those of the RSF-based models were 0.598, 0.680, and 0.727, respectively. The RSF-based model, including delta-radiomics features, significantly divided the cumulative incidence curves into two risk groups ($P < .05$). The feature map of the gray-level size-zone matrix showed that the difference in feature values between CECT and non-CECT images correlated with the incidence of DM.

Conclusions: Delta-radiomics features obtained from CECT and non-CECT images using RSF successfully predict the incidence of DM in patients with borderline resectable pancreatic carcinoma.

© 2024 The Author(s). Published by Elsevier Inc. on behalf of American Society for Radiation Oncology. This is an open access article under the CC BY-NC-ND license (http://creativecommons.org/licenses/by-nc-nd/4.0/).

Sources of support: This study was partially supported by the JSPS KAKENHI (grant number: 24K18827), the Foundation for Promotion of Cancer Research in Japan, and the Takeda Science Foundation.

The data are not publicly available due to privacy or ethical restrictions.

*Corresponding author: Mitsuhiro Nakamura, PhD.; Email: m_nkmr@kuhp.kyoto-u.ac.jp

https://doi.org/10.1016/j.adro.2024.101669

2452-1094/© 2024 The Author(s). Published by Elsevier Inc. on behalf of American Society for Radiation Oncology. This is an open access article under the CC BY-NC-ND license (http://creativecommons.org/licenses/by-nc-nd/4.0/).

Introduction

Pancreatic carcinoma (PC) remains the fourth leading cause of cancer-related deaths worldwide. PC has a poor prognosis, with a 5-year overall survival rate of less than 10%.[1] In patients with borderline resectable PC (BRPC), neoadjuvant concurrent chemoradiation therapy followed by pancreatectomy is a curative therapeutic option.[2,3] However, many patients with BRPC face early recurrence, mainly distant metastasis (DM) following pancreatectomy, which is associated with poor overall survival.[4] Despite this, there is no consensus regarding the prognostic prediction of DM for BRPC.[5] Therefore, the availability of an effective predictor of DM before or during the entire treatment would enable the identification of optimal multidisciplinary treatment strategies for BRPC.

The radiomics approach provides quantitative information from planning computed tomography (CT) images,[6] dose distribution,[7] and magnetic resonance (MR) images,[8] allowing the development of accurate prognostic prediction models for clinical decision-making. Specifically, delta-radiomics analysis, which employs changes in radiomics features in a set of corresponding images, has attracted increasing research attention.[9] Delta-radiomics features, identified using daily onboard volumetric images, can be used as noninvasive markers to monitor early treatment response during radiation therapy. Previous studies have reported that delta-radiomics features from daily CT and MR images predict early changes in treatment response in patients with resectable or BRPC[10] and those with locally advanced or BRPC,[11] respectively. As a novel application of the delta-radiomics approach, delta-radiomics features extracted from contrast-enhanced CT (CECT) and non-CECT images have been recently found to characterize tumor heterogeneity and predict the invasiveness of lung adenocarcinoma.[12] In patients with BRPC, the extent of contrast agents' infiltration into the tissue/tumor borders may be useful in predicting prognosis. However, no previous study has focused on predicting DM in patients with BRPC using delta-radiomics features calculated from CECT and non-CECT images.

Hence, in this study, we aimed to investigate the effectiveness of radiomics features obtained from CECT and non-CECT images and calculate these differences as delta-radiomics features for predicting DM in patients with BRPC. Toward this goal, we developed a predictive model of DM with clinical and radiomics features using Fine-Gray regression (FG) and random survival forest (RSF) techniques.

Methods and Materials

Study design and workflow

This retrospective study was approved by the appropriate institutional review board (approval number: R1446). Each patient provided written informed consent before the treatment.

Figure 1 illustrates the workflow of this study. The study involved 4 processes as follows: (1) data acquisition involving patient information retrieved from our institution's Digital Imaging and Communications in Medicine Radiation Therapy (DICOM-RT) files, including CECT, non-CECT images, and the gross tumor volume (GTV) structure; (2) compilation of clinical data, extraction of radiomics features from CECT and non-CECT images, and computation of delta-radiomics features using both images; (3) development of a predictive model of DM using FG and RSF with clinical features, converting selected radiomics features via 5-fold cross-validation after radiomics features to z scores, which represented the standardized values with a mean of zero and an SD of 1, and reducing the dimension of radiomics features; and (4) assessment of the model's accuracy using a nomogram by FG, feature importance analysis by RSF, and feature color maps.

Patients

A total of 250 patients with PC who underwent radiation therapy at our institution between February 2013 and December 2021 were evaluated. The patient selection flowchart is shown in Fig. E1. Overall, 67 patients with BRPC were eligible for this study (Fig. 1A). DM was defined as disease progression to other organs or peritoneal dissemination and was evaluated until death or the end of the study period, with patients censored accordingly. Patients lost to follow up were censored.

CT image acquisition

Non-CECT images were acquired during treatment planning with patients instructed to hold their breath at end-exhalation, and the images had a slice thickness of 2 mm. CECT images were immediately obtained under the same conditions. According to our hospital protocol, CECT images were acquired 40 seconds after intravenous contrast media administration at a rate of 2 mL/s.

After delineating the GTV, including the primary tumor and metastatic lymph nodes, by at least 2 board-certified radiation oncologists, the DICOM-RT files consisting of CECT and non-CECT images and structure of the GTVs were exported. The patients were treated with end-exhalation breath-holding at a prescribed dose of 42 Gy in 15 fractions. The details of the treatment strategy are summarized in our previous report.[13]

Feature collection and extraction

Before developing predictive models for DM, we collected clinical features and extracted radiomics features

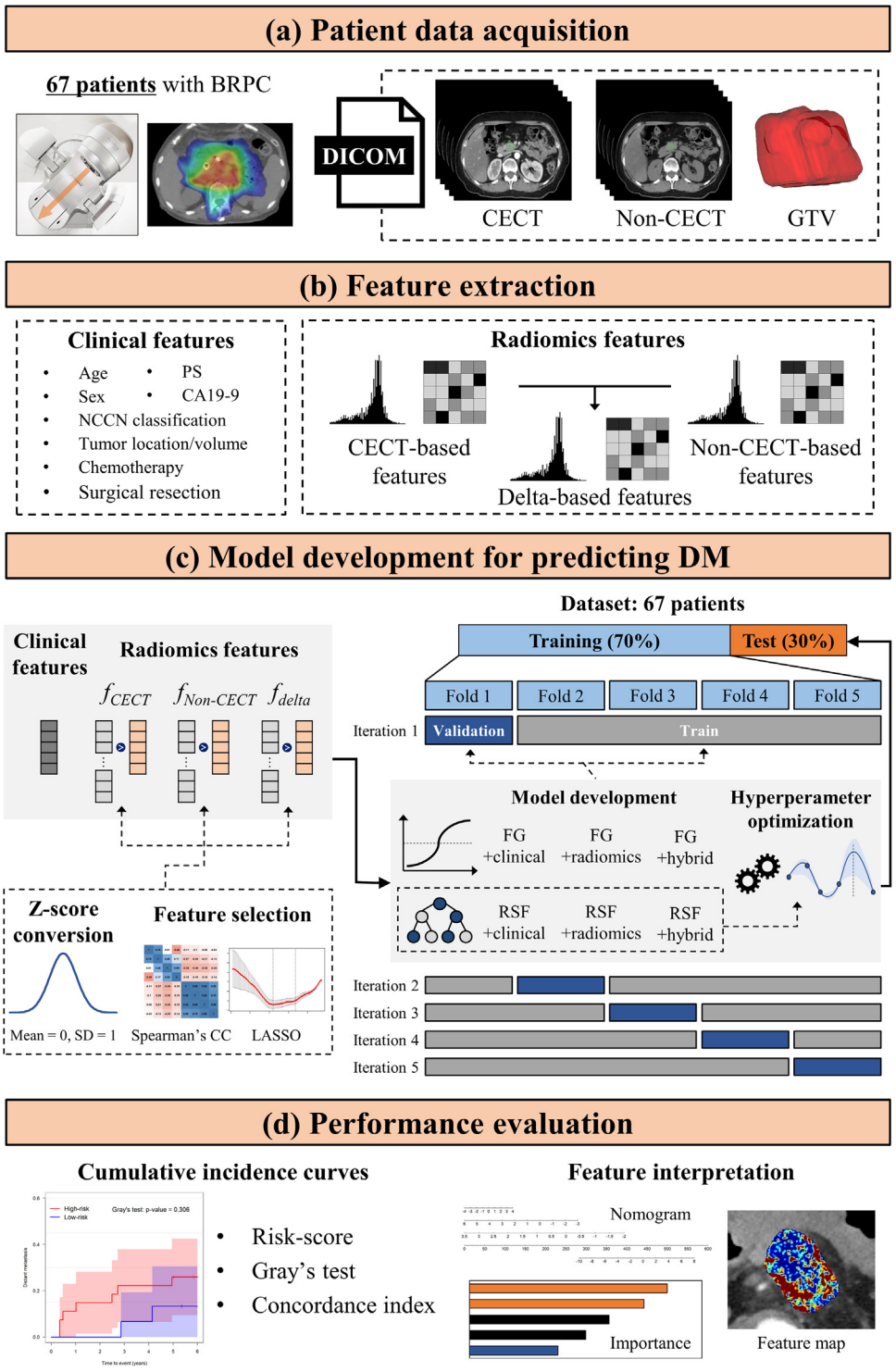

Figure 1 Study workflow.

Abbreviations: BRPC = borderline resectable pancreatic carcinoma; CA19-9 = carbohydrate antigen 19-9; CC = correlation coefficient; CECT = contrast-enhanced computed tomography; DICOM = Digital Imaging and Communications in Medicine Radiation Therapy; DM = distant metastasis; f_{CECT} = value of radiomics features extracted from CECT images; f_{delta} = subtracting the feature values based on CECT and non-CECT images; $f_{Non\text{-}CECT}$ = value of radiomics features extracted from non-CECT images; FG = Fine-Gray regression; GTV = gross tumor volume; LASSO = least absolute shrinkage and selection operator; NCCN = National Comprehensive Cancer Network; PS = performance status; RSF = random survival forest.

from CECT and non-CECT images (Fig. 1B). The clinical features included age, sex, performance status score, carbohydrate antigen 19-9 level, National Comprehensive Cancer Network guideline classification,[14] tumor location/volume, selection of induction/concurrent/maintenance chemotherapy, and surgical resection. For radiomics feature extraction, the DICOM-RT files were initially converted to nearly raw raster data files using a 3-dimensional slicer (version 4.10.2; Kitware Inc).[15] Next, 3906 radiomics features, comprising both CECT and non−CECT-based radiomics features, as well as delta-radiomics features, were extracted using the PyRadiomics software.[16] Delta-radiomics features (f_{delta}) were calculated as the difference in feature values between CECT and non-CECT images as follows

$$f_{delta} = f_{CECT} - f_{non-CECT}, \quad (1)$$

where f_{CECT} and $f_{non-CECT}$ denote the values of radiomics features extracted from the CECT and non-CECT images, respectively.[12]

For each category, the 1302 radiomics features consisted of 18 first-order-based, 75 texture-based, 465 (93 × 5) Laplacian of Gaussian (LoG)-based, and 744 (93 × 8) wavelet-based features (Table E1). The extracted features, such as the first-order, gray-level co-occurrence matrix, gray-level dependence matrix, gray-level run-length matrix, gray-level size-zone matrix (GLSZM), and neighboring-gray-tone difference matrix, were defined using the image biomarker standardization initiative.[17] The images underwent smoothing using a Gaussian filter, followed by convolution with a Laplacian filter to enhance the edges. The filter width was determined by sigma values of 0.5, 1.0, 1.5, 2.0, and 2.5 mm. The wavelet filters were based on the following 8 decompositions in the left-right, anterior-posterior, and superior-inferior directions: LLL, LLH, LHL, LHH, HLL, HHL, HLH, and HHH. The voxel of interest was defined as the GTV and the following parameters were set: a resampled voxel size of 1 × 1 × 1 mm^3 and a bin width of 25 Hounsfield units.[16]

Feature selection and model development

This study was categorized as "Type 2a: Random split-sample development and validation" in the Transparent Reporting of a multivariable prediction model for Individual Prognosis Or Diagnosis statement.[18] Before developing the predictive models for DM, all patients were randomly divided into the training (70%) and test (30%) data sets according to previous studies (Fig. 1C).[7,19] The radiomics features in the training data set were converted to z scores to assign different variables to the same scale. The f_{CECT}, $f_{non-CECT}$, and f_{delta} were normalized as follows

$$f_z = \frac{f - f_{mean}}{f_{SD}}, \quad (2)$$

where f_z is the converted feature value; f is the f_{CECT}, $f_{non-CECT}$, and f_{delta}; f_{mean} is the mean value of each feature type; and f_{SD} is the SD value of the feature type. Then, the features in the test data set were normalized based on the mean and SD of the training data set. Subsequently, the feature dimension was reduced using Spearman's correlation coefficient (CC) based on the redundancy between radiomics features.[20] When a radiomics feature exhibited a CC ≥ 0.80 with other features, the one with a greater number of remaining correlated features was eliminated.[7,20] Then, the least absolute shrinkage and selection operator (LASSO) was applied based on the regularization between the remaining radiomics features and clinical outcomes.[21] The hyperparameter λ in LASSO was optimized to minimize the cost function as the feature selection function.[21]

A total of 22 predictive models were developed as follows: with clinical features (clinical model); with delta-, CECT-, and non−CECT-based radiomics features (radiomics$_{all}$ model); with delta-based radiomics features (radiomics$_{delta}$ model); with CECT- and non−CECT-based radiomics features (radiomics$_{CECT/non-CECT}$ model); with CECT-based radiomics features (radiomics$_{CECT}$ model); with non−CECT-based radiomics features (radiomics$_{non-CECT}$ model); and with the combination of the abovementioned clinical and radiomics features (hybrid$_{all}$, hybrid$_{delta}$, hybrid$_{CECT/non-CECT}$, hybrid$_{CECT}$, and hybrid$_{non-CECT}$ model) using FG[22] and RSF[23] considering total death as the competing risk. In developing predictive models for BRPC, DM was set as the event of interest, and competing risks were considered using time-to-event data.[24] This is because competing risks can lead to an overestimation of risks associated with the primary event of interest. The optimal hyperparameters were determined using a stratified 5-fold cross-validation with a training data set for the RSF-based model. Subsequently, the 22 developed models were applied to the remaining test data sets, and the patients were divided into high- and low-risk groups based on their risk scores. The sum of the cumulative hazard functions with FG and RSF was calculated as patient-specific scores (Fig. 1D). The nomogram from FG and feature importance from RSF were calculated to interpret the meaning of radiomics features. The nomogram represents the graphical prediction score of the developed models based on traditional statistical methods, such as the FG algorithm.[22] In addition, the feature importance of the RSF model, which was identified by noizing the variables, indicated its contribution to model development.[23] Feature color maps were additionally generated using the voxel-based extraction function in PyRadiomics.[16]

Statistical analyses

The prognostic power of cumulative incidence curves was evaluated according to the concordance index (C-

index) instead of the area under the receiver operating characteristic curve to consider the time-dependent model performance. The 95% CIs were calculated using 2000 bootstrapping iterations. Additionally, the statistical significance between the high- and low-risk groups was evaluated using Gray's test.[21] An appropriate test was determined based on normality using the Shapiro-Wilk test. All statistical analyses were performed using R software version 4.3.0 (R Software for Statistical Computing).[25] Statistical significance was set at $P < .05$.

Results

Patient characteristics and outcomes

The median follow-up durations were 23.8 (range, 6.0-105.9), 23.4 (range, 6.4-105.9), and 30.9 (range, 6.0-100.8) months in the entire training and test data sets, respectively ($P = .462$, independent sample t test). In each data set, 47.8%, 45.7%, and 52.4% of patients, respectively, were alive at the time of analysis ($P = .793$, Pearson contingency χ^2 tests). The incidence of DM after treatment in each data set was 70.1%, 69.6%, and 71.4%, respectively ($P = .999$, Pearson contingency χ^2 tests). The patient characteristics are summarized in Table 1.

Feature selection

Based on the Spearman CC, 397 of 3906 (10.2%), 276 of 1302 (21.2%), 146 of 2604 (5.6%), 82 of 1302 (6.3%), and 78 of 1302 features (6.0%) were not redundant with the other features for the radiomics$_{all}$, radiomics$_{delta}$, radiomics$_{CECT/non\text{-}CECT}$, radiomics$_{CECT}$, and radiomics$_{non\text{-}CECT}$ models (CC < 0.80), respectively. In adaptive LASSO, the remaining features were reduced to 8 of 3906 (0.20%), 10 of 1302 (0.77%), 8 of 2604 (0.31%), 10 of 1302 (0.77%), and 9 of 1302 (0.69%) for the radiomics$_{all}$, radiomics$_{delta}$, radiomics$_{CECT/non\text{-}CECT}$, radiomics$_{CECT}$, and radiomics$_{non\text{-}CECT}$ models, respectively.

Performance of the predictive model

For the training data sets, all FG- and RSF-based models showed significant differences in predicting the incidence of DM (Figs. E2 and E3, $P < .05$). Figures 2 and 3 show the curves for the test data sets. The C-indices of all RSF-based models were higher than those of the FG-based models. No FG-based models showed a significant prediction for DM ($P > .05$). In contrast, the RSF-based hybrid$_{all}$, hybrid$_{delta}$, radiomics$_{all}$, and radiomics$_{delta}$ models significantly divided the cumulative incidence curves of

Table 1 Patient characteristics

Characteristics	Description	Total ($N = 67$)	Train data set ($n = 46$)	Test data set ($n = 21$)	P value
Age (y)†	Median (range)	68 (46-85)	69 (46-78)	68 (53-85)	.806
Sex*	Male/female	38/29	29/17	9/12	.184
Performance status*	0/1	47/20	29/17	18/3	.085
NCCN classification*	BR-A/BR-PV/BR-A (PV)	34/10/23	24/7/15	10/3/8	.935
Tumor		-	-	-	-
Location*	Head-uncus/body-tail	44/23	31/15	13/8	.783
Volume (cm^3)†	Median (range)	27.0 (14.0-50.0)	27.0 (14.0-50.0)	25.0 (16.0-42.0)	.976
CA19-9 (U/mL)†	Median (range)	96.6 (0.0-4017.0)	105.97 (0.0-4017.0)	75.7 (0.6-1325.0)	.770
Chemotherapy					
Induction*	Gem or S-1/FOLFIRINOX or Gem + nabPTX	49/18	32/14	17/4	.388
Concurrent*	Gem/S-1	64/3	44/2	20/1	.999
Adjuvant*	Gem or S-1/none	42/25	28/18	14/7	.787
Surgical resection*	With/without	46/21	31/15	15/6	.785

$p < .05$ indicates significant differences in the train and test data sets.

Abbreviations: BR-A = borderline resectable with artery involvement; BR-A (PV) = borderline resectable with artery and portal vein involvement; BR-PV = borderline resectable with portal vein involvement; CA19-9 = carbohydrate antigen 19-9; Gem = gemcitabine; nabPTX = nab-paclitaxel; NCCN = National Comprehensive Cancer Network; S-1 = a combined drug of tegafur, gimestat, and otastat potassium.

*The sex, performance status, NCCN classification, tumor location, chemotherapy schedule, and surgical resection included the percentage or number of patients; the corresponding p values were determined using Pearson contingency χ^2 tests.

†The age, tumor volume, and CA19-9 included the median value (range, minimum to maximum); the corresponding p value was determined using an independent sample t test.

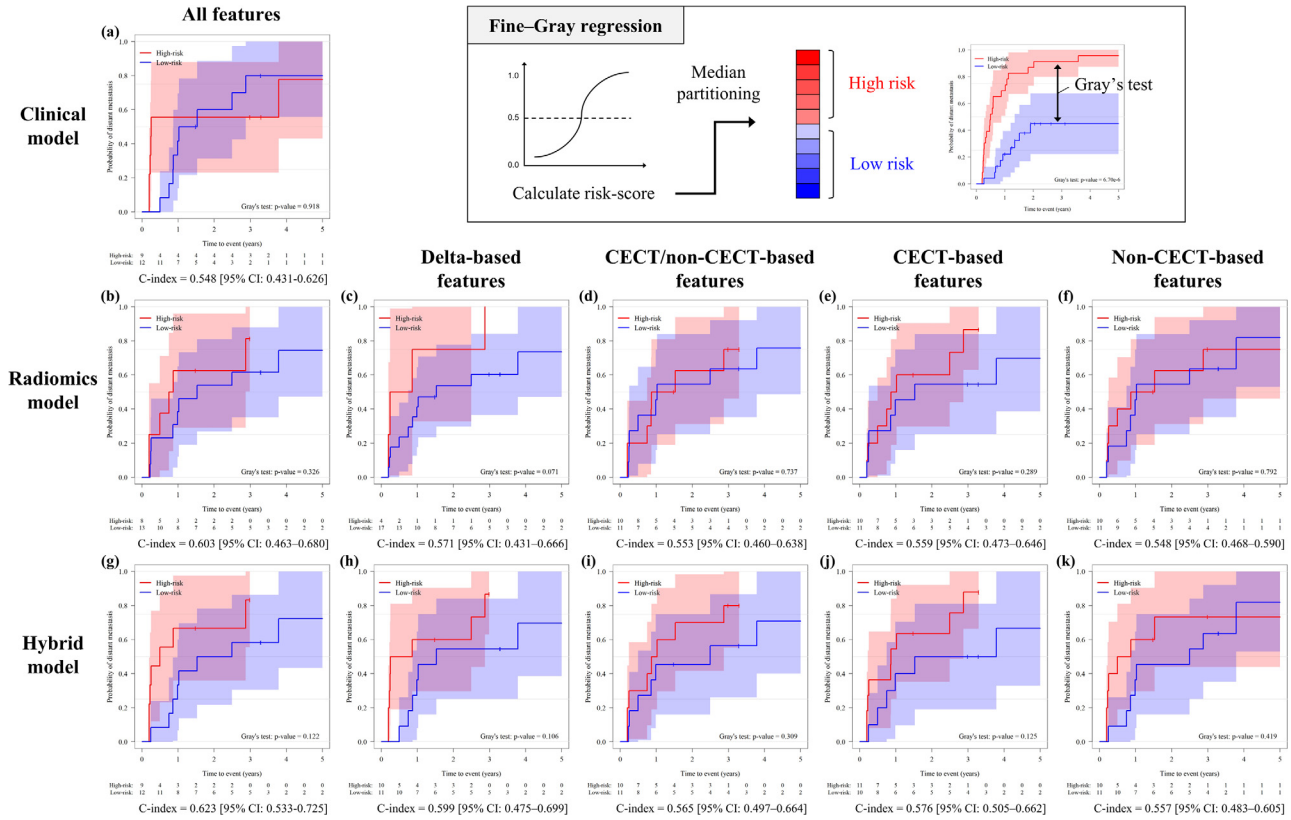

Figure 2 Cumulative incidence curves of the (A) clinical, (B-F) radiomics, and (G-K) hybrid models for test data sets using Fine-Gray regression. Each curve is derived from (A, B, G) all, (C, H) delta-based, (D, I) contrast-enhanced computed tomography (CECT)/non−CECT-based, (E, J) CECT-based, and (F, K) non−CECT-based features. The patients in the test data set are divided into high- and low-risk groups based on their risk scores calculated from the training data sets.
Abbreviations: C-index = concordance index.

DM ($P < .05$). The C-indices of the 3 radiomics and 3 hybrid models based on RSF were higher than that of the clinical model (C-index, 0.598 [95% CI, 0.532-0.746]). The model with the best performance was the hybrid$_{all}$ model (C-index, 0.727 [95% CI, 0.654-0.851]), followed by the hybrid$_{delta}$ model (C-index, 0.693 [95% CI, 0.628-0.815]). The performance metrics of developed models are summarized in Table E2 for the training data set and Table E3 for the test data set.

Feature interpretation for DM prediction

Figure 4 shows an example of a nomogram from the FG-based hybrid$_{all}$ model and the feature importance from the RSF-based hybrid$_{all}$ model. The clinical and radiomics$_{all}$ models are illustrated in Figs. E4 and E5. The nomogram showed that compared with clinical features, 3 radiomics features had a stronger influence on the predictive ability for DM in the FG-based hybrid$_{all}$ model. For the RSF-based feature importance, the "Delta LoG (sigma = 0.5 mm) GLSZM size zone nonuniformity" feature showed higher importance than the 11 clinical features, such as the surgical resection and adjuvant chemotherapy in the hybrid$_{all}$ model.

Figure 5 shows an example of a feature color map generated with "Delta LoG (sigma = 0.5 mm) GLSZM size zone nonuniformity" for patients with/without DM. The high-risk patients showed high values in the peripheral region of the tumors on CECT images, while the low-risk patients yielded visually similar feature maps on CECT and non-CECT images. In a representative patient with DM, the value of the above feature was higher compared with that of a representative patient without DM (52.6 vs 10.3).

Discussion

Previous studies on PC have primarily focused on predicting early treatment response using daily CT[10] and MR images,[11] as well as predicting lymph node metastases using CECT-based radiomics features.[26,27] To our knowledge, no studies have explored delta-radiomics analysis focusing on CECT and non-CECT images for predicting DM in BRPC.

In this study, we developed predictive models for DM in patients with BRPC using radiomics features extracted from CECT and non-CECT images, as well as delta-radiomics features calculated from both image types. The models showed that delta-radiomics features improved the

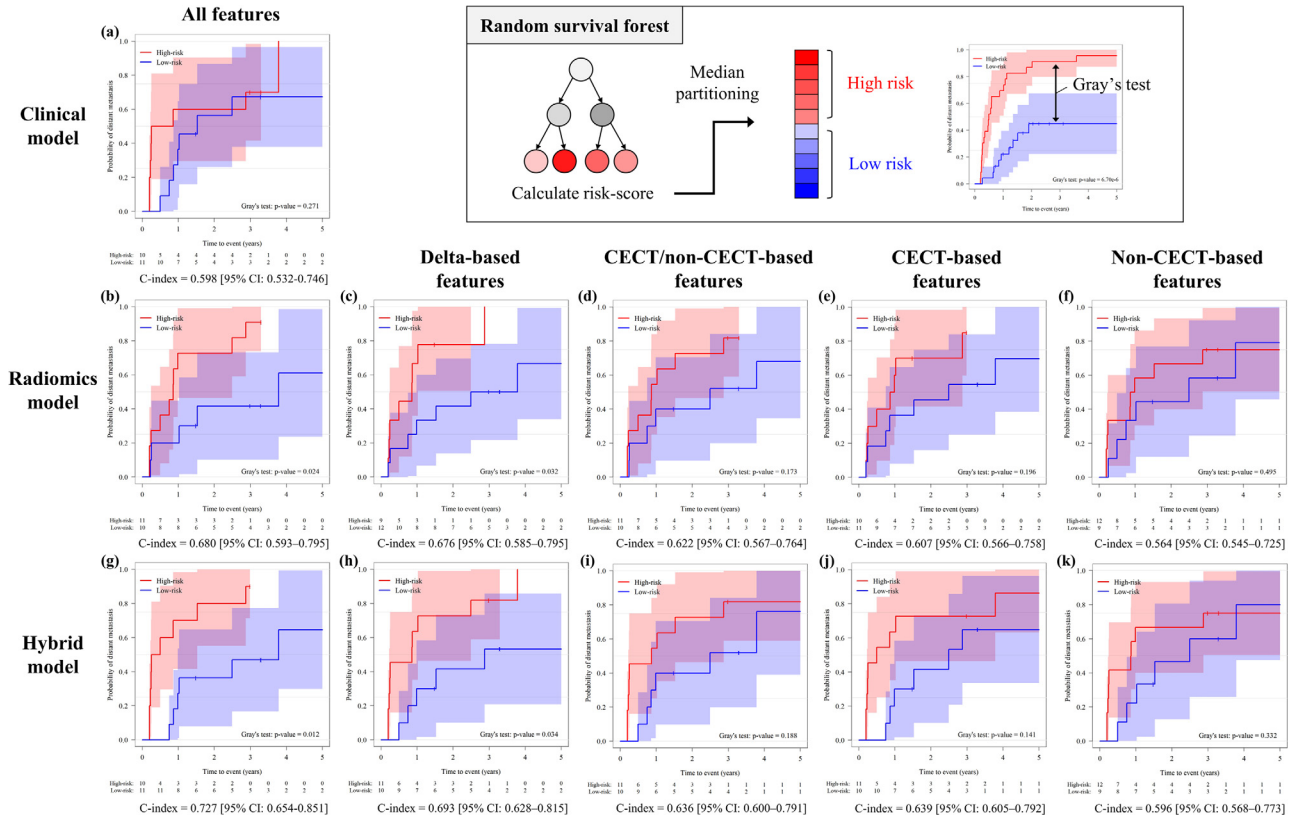

Figure 3 Cumulative incidence curves of the (A) clinical, (B-F) radiomics, and (G-K) hybrid models for test data sets using random survival forest. Each curve is derived from (A, B, G) all, (C, H) delta-based, (D, I) contrast-enhanced computed tomography (CECT)/non−CECT-based, (E, J) CECT-based, and (F, K) non−CECT-based features. The patients in the test data set are divided into high- and low-risk groups based on their risk scores calculated from the training data set.
Abbreviations: C-index = concordance index.

predictive ability for DM compared with clinical features by quantifying the extent of contrast agents' infiltration. Further, the predictive performance of radiomics$_{all}$, radiomics$_{delta}$, hybrid$_{all}$, and hybrid$_{delta}$, including delta-radiomics features, outperformed those without them, indicating that delta-radiomics features are more useful than a combination of radiomics features extracted solely from CECT and non-CECT images for predicting DM in patients with BRPC. These features can serve as noninvasive markers to determine optimal treatment strategies based on risk scores calculated from CECT and non-CECT images combined with clinical features, such as chemotherapy and surgical resection. Our findings provide a novel perspective for predicting DM, and the delta-radiomics approach has potential as a supporting strategy for clinical decision-making and individualizing radiation therapy in patients with BRPC.

The high accuracy of our models demonstrates the potential of our approach in prognostic prediction using delta-radiomics features from CECT and non-CECT images. Liu et al[28] analyzed the incidence of DM in patients with resectable PC and identified clinical features, such as age, sex, tumor size, alanine aminotransferase level, and carbohydrate antigen 19-9 level. They evaluated the model's performance using the receiver operating characteristic curve (area under the curve, 0.85). In addition, Shi et al[29] reported that a radiomics-based model combined with clinicopathologic characteristics and body composition measures could predict postresection survival in pancreatic ductal adenocarcinoma. They found that the radiomics model successfully divided the patients into high- and low-risk groups for predicting local recurrence and DM (P = .026). However, no previous study has analyzed the incidence of DM in BRPC using cumulative incidence curves and the C-index, which considers competing risks. Thus, it is not easy to compare our results directly with those of previous studies. A previous study predicted the incidence of DM using RSF-based models comprising CT-based radiomics features in patients with early-stage non-small cell lung cancer (NSCLC).[21] Although the incidence of DM differs between NSCLC and BRPC (15.6% vs 70.1%) cases, the C-index of our model was higher than that of previous studies (maximum C-index, 0.727 [95% CI, 0.654-0.851] vs 0.680 [95% CI, 0.550-0.810]). Addressing the challenge of imbalanced data sets is crucial to avoid bias toward the majority class. While high C-index values may indicate good predictive performance, they may not necessarily

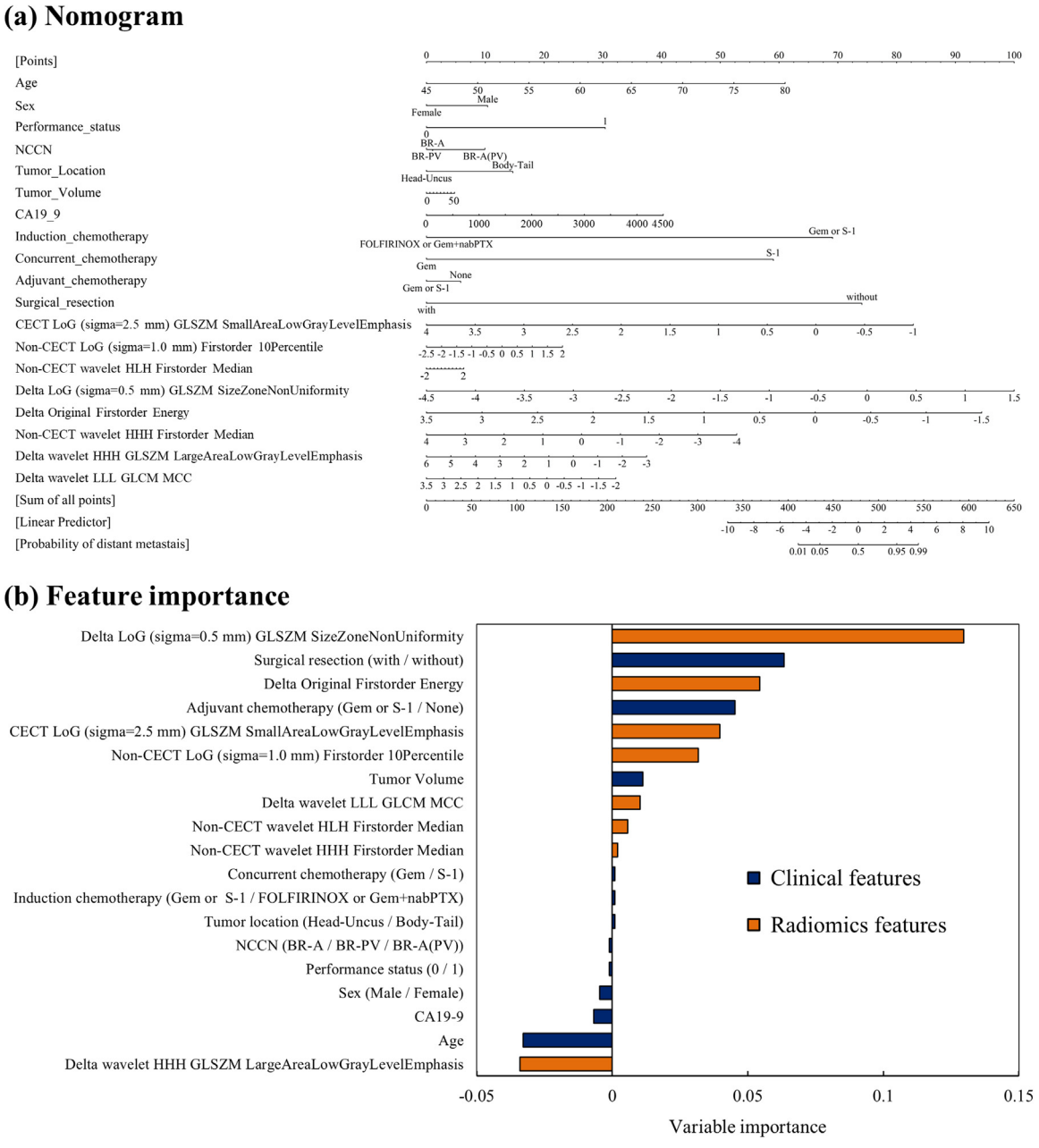

Figure 4 Example of (A) a nomogram from Fine-Gray regression and (B) feature importance from random survival forest in the hybrid$_{all}$ model. Negative values of feature importance indicate a random fluctuation.

Note: Wavelet filters are based on the following 8 decompositions in the left-right, anterior-posterior, and superior-inferior directions: LLL, LLH, LHL, LHH, HLL, HHL, HLH, and HHH.

Abbreviations: BR-A = borderline resectable with artery involvement; BR-A (PV) = borderline resectable with both artery and portal vein involvement; BR-PV = borderline resectable with portal vein involvement; CA19-9 = carbohydrate antigen 19-9; CECT = contrast-enhanced computed tomography; Gem = gemcitabine; GLCM = gray-level co-occurrence matrix; GLSZM = gray-level size-zone matrix; LoG = Laplacian of Gaussian; nabPTX = nab-paclitaxel; NCCN = National Comprehensive Cancer Network; S-1 = combined drug of tegafur, gimestat, and otastat potassium.

reflect high precision and recall because of this imbalance. In the current study, weighted average recall, precision, and f1 score were calculated to properly assess the predictive performance of imbalanced data sets. The results indicated that the hybrid$_{all}$ model with RSF accurately predicted the incidence of DM in 9 of 10 (90.0%) and 6 of 11 patients (54.5%) in the test data set in the high- and low-risk groups, respectively (P = .012). Despite the data set's imbalance, with a DM incidence of 70.1%, our approach successfully stratified patients into high- and low-risk groups using delta-radiomics features. Hence, to effectively predict the future incidence of DM, generating cumulative incidence curves using appropriate evaluation metrics and statistical tests is essential.

Our results showed that the RSF-based predictive model outperformed the FG-based model. A previous

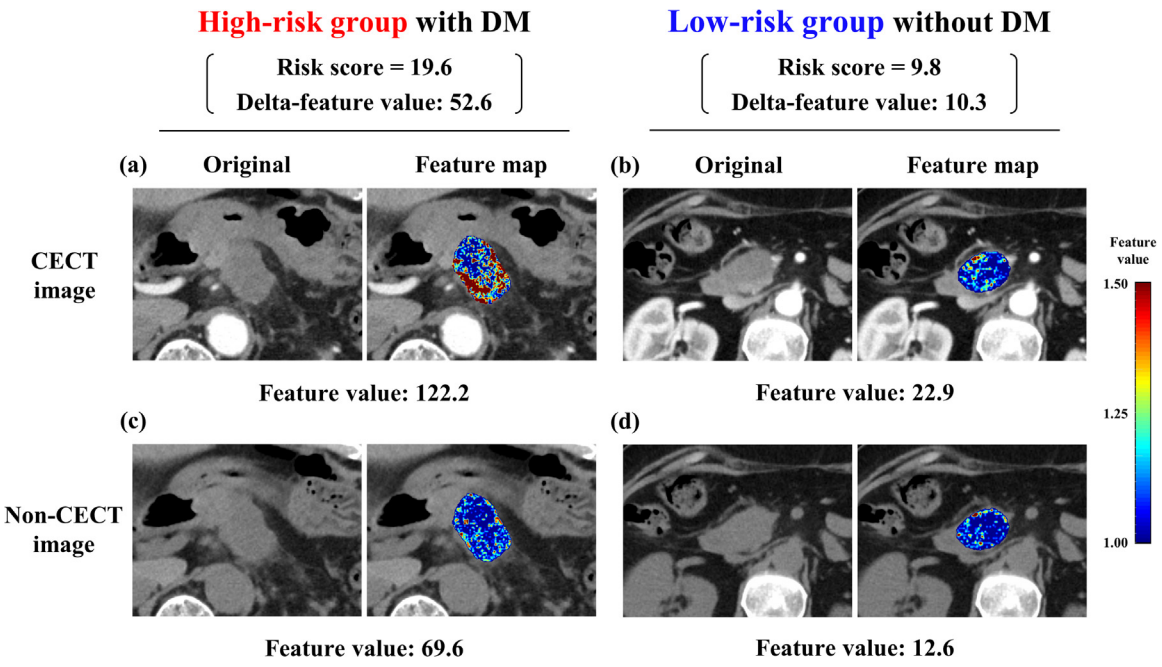

Figure 5 Example of a feature color map, contrast-enhanced computed tomography (CECT) images, and non-CECT images in patients with and without distant metastasis (DM). (A, C) The cases of a high-risk patient who has developed DM at 90 days and (B, D) low-risk patients who are censored without DM at 1200 days after the start of radiation therapy are presented. The median risk score for the hybrid$_{all}$ model with random survival forest was 17.9.

study reported that the predictive performance of the RSF model was superior to that of the FG model when a complex relationship existed between the outcome and predictor variables.[30] Although RSF can be used to develop predictive models with high accuracy, hyperparameter optimization is essential for achieving maximum performance with high robustness.[21] Therefore, before developing RSF-based models using radiomics features, the appropriate study designs and methodologies should be selected.

Our results also indicated that clinical models successfully predicted early DM development within 3 months in the high-risk group compared with the radiomics model. One possible reason for this is that the treatment strategy for BRPC sometimes did not include surgical resection or maintenance chemotherapy because of the early disease progression, including DM.[13] These 2 clinical features have been identified as important features in RSF-based clinical and hybrid$_{all}$ models. However, the radiomics features predicted the development of DM even after 3 months, and the hybrid model combining them with clinical features successfully partitioned the cumulative incidence curve into high- and low-risk groups at all time points. Therefore, the prediction of DM with clinical and radiomics features allows it to detect DM and change the treatment strategy earlier in patients with BRPC undergoing multimodality therapy.

The feature importance determined in the RSF-based model clarifies the contribution of radiomics features to model development. The hybrid$_{all}$ model with RSF, which had the best predictive ability, showed that the "Delta LoG (sigma = 0.5 mm) GLSZM size zone nonuniformity" feature was the most important feature for predicting DM of BRPC. Although the target organs and imaging modalities differ, the usefulness of GLSZM features has been reported.[11,19] Simpson et al[11] found that the delta-based "GLSZM large zones low gray-level emphasis" features contributed to the predictive ability for treatment response based on MR images in patients with locally advanced or BRPC. Zhu et al[19] showed that when developing models to predict DM in esophageal cancer, the important CT-based radiomics features include wavelet filter-based GLSZM features. The types of selected radiomics features are partially consistent with those of previous studies; however, the interpretation of the features has not been discussed, making comparison with our results difficult.

For the implications of the abovementioned radiomics features, our study showed that the "Delta LoG (sigma = 0.5 mm) GLSZM size zone nonuniformity" feature represented the differences in the distribution of contrast agents within the tumor on feature maps. GLSZM quantifies the areas of neighboring pixels with the same gray level in the voxel of interest.[17] Given that the tumor periphery of the high-risk patient exhibited contiguously high values on CECT-based feature maps, the difference between CECT and non-CECT images was enhanced by the LoG filter, which contributed to the highly accurate prediction of DM. However, in a previous multi-institutional phantom study, using LoG filters reduced the

reproducibility of radiomics features from onboard volumetric images under different imaging conditions.[31] Thus, after exploring the acceptability of the selected radiomics features, future studies should investigate reproducible radiomics features with high accuracy for prognostic prediction.

Our study focused on CECT and non-CECT images and their differences in identifying radiomics features within the GTVs. Meanwhile, previous studies have reported the effectiveness of radiomics features extracted from MR images for prognostic prediction in PC.[11,32] Although MR images provide superior soft-tissue contrast to cone beam CT (CBCT) images, Ogawa et al[33] demonstrated the possibility of delineating GTVs on kilovoltage CBCT images obtained during online adaptive radiation therapy. Therefore, the use of delta-radiomics features from onboard volumetric images, such as those from MR and CBCT, may improve the predictive ability for DM in patients with PC.

This study had some limitations that should be considered when interpreting the findings. First, the study had a retrospective design, included a limited sample size, and was conducted at a single institution. This may have caused potential bias in patient characteristics and outcomes. Simultaneously, special attention was required in the model development, including the feature selection by a linear model and hyperparameter optimization, to avoid overfitting the training data set.[21] It was challenging to obtain a sufficient number of patients with PC, as previous studies included only 90[10] and 30 patients.[11] Although the number of eligible patients in this study was not significantly different from that of other studies, our findings should be externally validated using a large multicenter cohort. However, we also established the accuracy of the proposed results by calculating the 95% CI using bootstrap iterations. Second, similar to previous studies, the current study did not include daily onboard volumetric images.[10,11] The addition of the above images, such as CBCT images, to the model development may yield different predictive results. Regardless of the abovementioned limitations, our findings indicate that delta-radiomics analysis focused on planning CECT and non-CECT images has the potential to predict DM with high accuracy. Therefore, this study could provide a perspective for improving the clinical treatment strategy. Third, we only considered some treatment processes, such as chemotherapy and surgical resection. However, the duration and amount of chemotherapy and details of surgical resection are highly dependent on the treatment protocol or performance status of patients, making it difficult to include these details in the current study owing to the limited sample size. Fourth, the study did not investigate the differences in radiomics features related to the contrast agents used. Although Hou et al[34] reported that radiomics features from CECT images can predict the treatment response in esophageal carcinoma, and Kakino et al[35] showed that using a contrast agent reduced the reproducibility of radiomics features in patients with NSCLC. However, the protocol for CECT depends on patient characteristics. Therefore, it is essential to investigate the effects of different imaging protocols on radiomics features to perform a standardized radiomics analysis of CECT images.

Conclusions

The present study developed predictive models for DM using clinical and radiomics features extracted from CECT and non-CECT images in patients with BRPC. When radiomics features were combined with clinical features, the RSF-based model showed better predictive performance for DM than the FG-based model. Specifically, a model that included delta-radiomics with RSF was successfully used to divide the cumulative incidence curves of DM and identify high- and low-risk patients based on their risk scores. Furthermore, after quantifying the distribution of contrast regions within the tumor using delta-radiomics features, the radiomics-based feature maps calculated from CECT and non-CECT images correlated with the incidence of DM. This novel methodology of delta-radiomics for predicting DM in patients with BRPC can be clinically significant by integrating the interpretation of radiomics features. Furthermore, our delta-radiomics approach may help individualize clinical decision-making for neoadjuvant therapy in patients with BRPC.

Disclosures

None.

Acknowledgments

We sincerely appreciate all the staff and members of the Medical Physics Laboratory of Kyoto University Graduate School of Medicine (http://medicalphysics.hs.med.kyoto-u.ac.jp/) for their excellent technical support and valuable comments on this study.

Supplementary materials

Supplementary material associated with this article can be found in the online version at doi:10.1016/j.adro.2024.101669.

References

1. Siegel RL, Miller KD, Wagle NS, Jemal A. Cancer statistics, 2023. *CA Cancer J Clin*. 2023;73:17-48.
2. Mizrahi JD, Surana R, Valle JW, Shroff RT. Pancreatic cancer. *Lancet*. 2020;395:2008-2020.
3. Rossi ML, Rehman AA, Gondi CS. Therapeutic options for the management of pancreatic cancer. *World J Gastroenterol*. 2014;20:11142-11159.
4. Nishio K, Kimura K, Amano R, et al. Preoperative predictors for early recurrence of resectable pancreatic cancer. *World J Surg Oncol*. 2017;15:16.
5. Hu JX, Zhao CF, Chen WB, et al. Pancreatic cancer: A review of epidemiology, trend, and risk factors. *World J Gastroenterol*. 2021;27:4298-4321.
6. Abunahel BM, Pontre B, Kumar H, Petrov MS. Pancreas image mining: A systematic review of radiomics. *Eur Radiol*. 2021;31:3447-3467.
7. Adachi T, Nakamura M, Shintani T, et al. Multi-institutional dose-segmented dosiomic analysis for predicting radiation pneumonitis after lung stereotactic body radiation therapy. *Med Phys*. 2021;48:1781-1791.
8. Li G, Li L, Li Y, et al. An MRI radiomics approach to predict survival and tumour-infiltrating macrophages in gliomas. *Brain*. 2022;145:1151-1161.
9. Nardone V, Reginelli A, Grassi R, et al. Delta radiomics: A systematic review. *Radiol Med*. 2021;126:1571-1583.
10. Nasief H, Zheng C, Schott D, et al. A machine learning based delta-radiomics process for early prediction of treatment response of pancreatic cancer. *npj Precis Oncol*. 2019;3:25.
11. Simpson G, Jin W, Spieler B, et al. Predictive value of delta-radiomics texture features in 0.35 Tesla magnetic resonance setup images acquired during stereotactic ablative radiotherapy of pancreatic cancer. *Front Oncol*. 2022;12: 807725.
12. Chen W, Wang R, Ma Z, et al. A delta-radiomics model for preoperative prediction of invasive lung adenocarcinomas manifesting as radiological part-solid nodules. *Front Oncol*. 2022;12: 927974.
13. Masui T, Nagai K, Anazawa T, et al. Impact of neoadjuvant intensity-modulated radiation therapy on borderline resectable pancreatic cancer with arterial abutment; a prospective, open-label, phase II study in a single institution. *BMC Cancer*. 2022;22(1):119.
14. Network NCC. NCCN clinical practice guidelines in oncology (NCCN guidelines). Accessed October 28, 2023. https://www.nccn.org/professionals/physician_.
15. Fedorov A, Beichel R, Kalpathy-Cramer J, et al. 3D Slicer as an image computing platform for the Quantitative Imaging Network. *Magn Reson Imaging*. 2012;30:1323-1341.
16. van Griethuysen JJM, Fedorov A, Parmar C, et al. Computational radiomics system to decode the radiographic phenotype. *Cancer Res*. 2017;77:e104-e107.
17. Hatt M, Vallieres M, Visvikis D, Zwanenburg A. IBSI: An international community radiomics standardization initiative. *J Nucl Med*. 2018;59:287.
18. Collins GS, Reitsma JB, Altman DG, Moons KG. Transparent reporting of a multivariable prediction model for individual prognosis or diagnosis (TRIPOD): The TRIPOD statement. *BMJ*. 2015;350:g7594.
19. Zhu C, Mu F, Wang S, Qiu Q, Wang S, Wang L. Prediction of distant metastasis in esophageal cancer using a radiomics–clinical model. *Eur J Med Res*. 2022;27:272.
20. Lv W, Yuan Q, Wang Q, et al. Radiomics analysis of PET and CT components of PET/CT imaging integrated with clinical parameters: Application to prognosis for nasopharyngeal carcinoma. *Mol Imaging Biol*. 2019;21:954-964.
21. Kakino R, Nakamura M, Mitsuyoshi T, et al. Application and limitation of radiomics approach to prognostic prediction for lung stereotactic body radiotherapy using breath-hold CT images with random survival forest: A multi-institutional study. *Med Phys*. 2020;47:4634-4643.
22. Lu Y, Zhou Y, Cao Y, Shi Z, Meng Q. A competing-risks nomogram in patients with metastatic pancreatic duct adenocarcinoma. *Med Sci Monit*. 2019;25:3683-3691.
23. Ishwaran H. Variable importance in binary regression trees and forests. *Electr J Stat*. 2007;1:519-537.
24. Austin PC, Lee DS, Fine JP. Introduction to the analysis of survival data in the presence of competing risks. *Circulation*. 2016;133:601-609.
25. R Core Team. *R: A language and environment for statistical computing*. Vienna, Austria: R Foundation for Statistical Computing; 2018.
26. Fang WH, Li XD, Zhu H, et al. Resectable pancreatic ductal adenocarcinoma: Association between preoperative CT texture features and metastatic nodal involvement. *Cancer Imaging*. 2020;20:17.
27. Li K, Yao Q, Xiao J, et al. Contrast-enhanced CT radiomics for predicting lymph node metastasis in pancreatic ductal adenocarcinoma: A pilot study. *Cancer Imaging*. 2020;20:12.
28. Liu X, Fu Y, Chen Q, et al. Predictors of distant metastasis on exploration in patients with potentially resectable pancreatic cancer. *BMC Gastroenterol*. 2018;18:168.
29. Shi H, Wei Y, Cheng S, et al. Survival prediction after upfront surgery in patients with pancreatic ductal adenocarcinoma: Radiomic, clinic-pathologic and body composition analysis. *Pancreatology*. 2021;21:731-737.
30. Nasejje JB, Whata A, Chimedza C. Statistical approaches to identifying significant differences in predictive performance between machine learning and classical statistical models for survival data. *PLoS One*. 2022;17: e0279435.
31. Adachi T, Nakamura M, Iramina H, et al. Identification of reproducible radiomic features from on-board volumetric images: A multi-institutional phantom study. *Med Phys*. 2023;50:5585-5596.
32. Xu X, Qu J, Zhang Y, Qian X, Chen T, Liu Y. Development and validation of an MRI-radiomics nomogram for the prognosis of pancreatic ductal adenocarcinoma. *Front Oncol*. 2023;13: 1074445.
33. Ogawa A, Nakamura M, Iramina H, Yoshimura M, Mizowaki T. Potential utility of cone-beam CT-guided adaptive radiotherapy under end-exhalation breath-hold conditions for pancreatic cancer. *J Appl Clin Med Phys*. 2023;24:e13827.
34. Hou Z, Ren W, Li S, et al. Radiomic analysis in contrast-enhanced CT: Predict treatment response to chemoradiotherapy in esophageal carcinoma. *Oncotarget*. 2017;8:104444-104454.
35. Kakino R, Nakamura M, Mitsuyoshi T, et al. Comparison of radiomic features in diagnostic CT images with and without contrast enhancement in the delayed phase for NSCLC patients. *Phys Med*. 2020;69:176-182.